Structural Engineering and Mechanics, *Vol. 47, No. 5 (2013) 713-727*
DOI: http://dx.doi.org/10.12989/sem.2013.47.5.713

PSO algorithm for fundamental frequency optimization of fiber metal laminated panels

H. Ghashochi-Bargh* and M.H. Sadr[a]

Aerospace Engineering Department, Centre of Excellence in Computational Aerospace Engineering, Amirkabir University of Technology, Hafez Avenue, Tehran, Iran

(Received March 16, 2013, Revised August 14, 2013, Accepted August 31, 2013)

Abstract. In current study, natural frequency response of fiber metal laminated (FML) fibrous composite panels is optimized under different combination of the three classical boundary conditions using particle swarm optimization (PSO) algorithm and finite strip method (FSM). The ply angles, numbers of layers, panel length/width ratios, edge conditions and thickness of metal sheets are chosen as design variables. The formulation of the panel is based on the classical laminated plate theory (CLPT), and numerical results are obtained by the semi-analytical finite strip method. The superiority of the PSO algorithm is demonstrated by comparing with the simple genetic algorithm.

Keywords: fiber metal laminated panel; particle swarm optimization algorithm; fundamental frequency

1. Introduction

Panel structures are widely used as structural components in various branches of engineering such as aerospace, civil and marine engineering. The usage of fiber metal laminates (FML) in these panel structures is increasing day to day and taking the place of traditional composites, due to their superior mechanical characteristics. FMLs consist of alternating layers of reinforced polymeric composites and metal sheets (aluminium, magnesium and/or titanium) in a way that metal sheets are outer layers protecting the inner composite layers without taking the poor fatigue strength of metal sheets and the poor impact strength of carbon fibers (or some composites). Advantages of FML can be listed as excellent fatigue behavior, superior impact resistance, inherent resistance to corrosion and environmental conditions, good fire resistance, low moisture absorption, weight reduction and improved damage tolerance characteristics (Aksoylar *et al*. 2012, Shooshtari and Razavi 2012, 2010, Ghashochi Bargh and Sadr 2011). In view of this, lay-up sequence optimization of inner composite layers has a significant role in improving the specific design objectives.

Also the concept of design and optimization of the constitutive material is established as a fundamental step in the process of design and optimization of composite structure (Gürdal *et al*. 1999). In this area, several researches have contributed with various partial results and/or

*Corresponding author, Ph.D. Candidate, E-mail: Ghashochi.b@aut.ac.ir
[a]Associate Professor, E-mail: Sadr@aut.ac.ir

http://www.techno-press.org/?journal=sem&subpage=8 ISSN: 1225-4568 (Print), 1598-6217 (Online)

characteristics of lamination parameters. Among these, the first to mention should naturally be (Tsai and Pagano 1968) who introduced the lamination parameters. (Fukunaga and Sekine 1992) determined the relationship between the four in-plane parameters and also for the four out-of-plane parameters. (Grenestedt and Gudmundson 1993) also determined that the application of lamination parameters as design variables in stiffness related optimization would produce a convex design space. (Bloomfield *et al*. 2009) developed an efficient method for optimization of composite structures in such a way that the non-convex nature of the problem is overcome. They established the feasibility constraints of the lamination parameters for a set of laminates with homogenous material but different angular orientations of each layer. Among first works on optimization of natural frequency in laminated composite materials, one can refer to Bert (1977), where presented results for the maximum fundamental frequency of a simply supported symmetric balanced laminate with a lay-up configuration of $[\pm\theta]_S$. Bert (1978) also proposed a suitable equation to determine the fundamental frequencies of composite plates with clamped boundaries. When considering four plies, he found that the optimal fiber orientation varied from 0 to 90 with increase in the plate aspect ratio. Kam and Chang (1993) traced the optimal lamination arrangement of thick composite plates for maximum buckling load and vibration frequency. Mateus *et al*. (1991) studied the optimal design of thin laminated plates and obtained results for maximum fundamental frequency and minimum elastic strain energy using finite element method to determine the frequency response. Narita (2003) offered a Ritz-based layerwise optimization approach for the symmetrical composite plates with respect to fiber orientation. Reiss and Ramachandran (1987) obtained the optimum design using a closed-form solution for the laminate frequency. Apalak *et al*. (2008) determined the optimal layer sequences of the symmetrical composite plates using Genetic Algorithm, artificial neural networks and finite element method. Fundamental frequency optimization of laminated composite panels is studied by Ghashochi and Sadr (2010, 2011, 2012) using Elitist-Genetic algorithm, particle swarm optimization algorithm and finite strip method. They (2011) also studied the optimal design of FMLs plate and obtained results for maximum fundamental frequency using Elitist-Genetic algorithm.

The objective of the present study is to find the optimum stacking sequence of inner composite layers of FML plates that gives the maximum natural frequency using particle swarm optimization (PSO) algorithm and finite strip method (FSM). The geometry of a typical finite strip of layered fiber metal is shown in Fig. 1 indicating the coordinate axes system pertaining to the strip

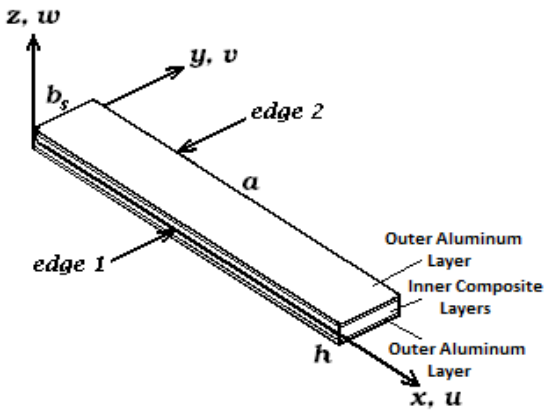

Fig. 1 Strip geometry of a layered fiber metal and coordinate axes system

displacements *u*, *v* and *w* with a length of *a* and width of b_s. The classical laminated plate (CLPT) theory is used for the finite strip formulation of the laminated plates. Finally, the effect of different panel aspect ratio, ply angles, number of layers and boundary conditions on the optimal designs is investigated.

2. Formulation

In the present study, we consider a rectangular FML plate with uniform total thickness *h* composed of *n* isotropic and orthotropic layers. The FML composite plate is assumed to be thin (*h/a=0.01*) so that the classical laminated plate theory (CLPT) is employed to analyse the problem and the following displacement field is assumed (Jones 1975, Vinson and Sierakowski 1986)

$$\begin{aligned}\bar{u}(x,y,z,t) &= u(x,y,t) - z\frac{\partial w(x,y,t)}{\partial x}\\ \bar{v}(x,y,z,t) &= v(x,y,t) - z\frac{\partial w(x,y,t)}{\partial y}\\ \bar{w}(x,y,z,t) &= w(x,y,t)\end{aligned} \tag{1}$$

where $\bar{u}, \bar{v}$ and $\bar{w}$ are the displacement components along the *(x, y, z)* coordinate directions of a point on the midplane, respectively.

The membrane strains ε and the bending curvatures ψ are defined as follows

$$\begin{Bmatrix}\bar{\varepsilon}_x\\ \bar{\varepsilon}_y\\ \bar{\gamma}_{xy}\end{Bmatrix} = \varepsilon + z\psi = \begin{Bmatrix}u_{,x}\\ v_{,y}\\ u_{,y}+v_{,x}\end{Bmatrix} + z\begin{Bmatrix}-w_{,xx}\\ -w_{,yy}\\ -2w_{,xy}\end{Bmatrix} \tag{2}$$

Here, a subscript after the comma denotes differentiation with respect to the variable following the comma. The stress resultants N_x, N_y and N_{xy} and the moment resultants M_x, M_y and M_{xy} are defined as follows

$$\begin{Bmatrix}N_x\\ N_y\\ N_{xy}\\ M_x\\ M_y\\ M_{xy}\end{Bmatrix} = \int_{-h/2}^{h/2}\begin{Bmatrix}\bar{\sigma}_x\\ \bar{\sigma}_y\\ \bar{\tau}_{xy}\\ z\bar{\sigma}_x\\ z\bar{\sigma}_y\\ z\bar{\tau}_{xy}\end{Bmatrix}dz = \begin{bmatrix}[A] & [B]\\ [B] & [D]\end{bmatrix}\times\begin{Bmatrix}\{\varepsilon\}\\ \{\psi\}\end{Bmatrix} \tag{3}$$

where *[A],[B]* and *[D]* are the matrices of extensional, coupling and bending stiffness coefficients defined by

$$[A] = \begin{bmatrix}A_{11} & A_{12} & A_{16}\\ A_{12} & A_{22} & A_{26}\\ A_{16} & A_{26} & A_{66}\end{bmatrix}, [B] = \begin{bmatrix}B_{11} & B_{12} & B_{16}\\ B_{12} & B_{22} & B_{26}\\ B_{16} & B_{26} & B_{66}\end{bmatrix}, [D] = \begin{bmatrix}D_{11} & D_{12} & D_{16}\\ D_{12} & D_{22} & D_{26}\\ D_{16} & D_{26} & D_{66}\end{bmatrix} \tag{4a}$$

The panel stiffness coefficients in Eq. (3) are determined by

$$(A_{ij}, B_{ij}, D_{ij}) = \sum_{k=1}^{n} \int_{zk-1}^{zk} (\overline{Q}_{ij})_k (1, z, z^2) dz, \quad i, j = 1, 2, 6 \tag{4b}$$

Because of the symmetry condition about the mid surface of the subject laminates, the in plane and out of plane coupling stiffness coefficients (B_{ij}) are zero.

According to the Hamilton principle, among possible motions of a system of particles which are consistent with constraints, the motion which gives a stationary value to the following integral will be happened

$$\int_{t_0}^{t_1} (T - U) dt \tag{5}$$

where T is the kinetic and U is the potential energy of the system. The governing equations are obtained by applying Lagrange equations of motion as (Apalak *et al*. 2008)

$$\frac{d}{dt}\left\{\frac{\partial L}{\partial \dot{d}}\right\} - \left\{\frac{\partial L}{\partial d}\right\} = \{0\} \tag{6}$$

where $L=T-U$, d is the nodal displacement and $\dot{d}$ is the nodal velocity. Here, the strain energy per unit volume is

$$U_s = \frac{1}{2} \overline{\sigma}^T \overline{\varepsilon} \tag{7}$$

using Eqs. (3)-(7) and integrating through the thickness of the structure with respect to z gives an expression for the strain and kinetic energies of each finite strip of the structure which was divided into S strips can written as

$$U_s = \frac{1}{2} \iint \{\varepsilon^T . [A] . \varepsilon + \psi^T . [D] . \psi\} dxdy \tag{8}$$

$$T_s = \frac{1}{2} \rho h \iint \{\dot{u}^2 + \dot{v}^2 + \dot{w}^2\} dxdy \tag{9}$$

where ρ is a mean mass per unit area of the plate.

For the complete panel, the total strain energy and kinetic energy are obtained by summations of the corresponding energy components of all strips. In this way, the whole structural matrices are generated by following the standard FEM assembly procedure and the structural equation of motions can be obtained by applying the Lagrange equations as (Apalak *et al*. 2008)

$$[M]\{\ddot{\overline{d}}\} + [K]\{\overline{d}\} = \{0\} \tag{10}$$

Therefore, eigenvalue problem for the vibration analysis can be obtained as

$$[[K] - \omega^2 [M]]\{\Theta\} = \{0\} \tag{11}$$

where ω and $\{\Theta\}$ are the natural frequency in rad/sec and the vibration mode shape, respectively.

Normalized natural frequency is

$$\Omega = \omega a^2 \left(\frac{\rho}{D_0}\right)^{1/2} \tag{12}$$

where the reference bending rigidity is

$$D_0 = {E_2 h^3}\Big/{12(1-\nu_{12}\nu_{21})} \tag{13}$$

The main objective in the optimization problem is to determine the optimal layer sequences which maximize the normalized frequency Ω for the first natural mode of the FML composite panel. It should be observed that the symmetry requirement it easily enforced by optimizing only one half of the laminate and deriving from symmetry conditions the other half. The optimization problem can be defined as

$$\begin{aligned} &\textit{Find} \qquad \theta = (Al, \theta_1, ..., \theta_k) \\ &\textit{Maximize} \quad \Omega = \Omega(Al, \theta_1, ..., \theta_k) \\ &\textit{Subject to} \quad -90^0 \le \theta_n \le 90^0 \end{aligned} \tag{14}$$

where *k* is half of the inner composite layers number. The optimal stacking sequences and ply angles are searched with the particle swarm optimization algorithm.

The assumed in-plane displacement and out-of-plane displacement in the full-energy semi-analytical finite strip method are (Sadr and Ghashochi Bargh 2010, 2011, 2012)

$$\begin{aligned} u &= \sum_{i=1}^{ru} ((1-\eta)u_{1i} + \eta u_{2i}) \cos(i\zeta x) \\ v &= \sum_{i=1}^{rv} ((1-\eta)v_{1i} + \eta v_{2i}) \sin(i\zeta x) \\ w &= \sum_{i=1}^{rw} ((1-3\eta^2+2\eta^3)w_{1i} + b_s(\eta - 2\eta^2 + \eta^3)\theta_{1i} \\ &\quad + (3\eta^2 - 2\eta^3)w_{2i} + b_s(\eta^3 - \eta^2)\theta_{2i})W_i(x) \\ W_i(x) &= \begin{cases} \sin(i\zeta x) & \textit{end simply sup ported} \\ \sin(\zeta x).\sin(i\zeta x) & \textit{end clamped} \end{cases} \end{aligned} \tag{15}$$

Where u_{1i}, u_{2i}, v_{1i} and v_{2i} are the undetermined in-plane nodal displacement parameters and w_{1i}, w_{2i}, θ_{1i} and θ_{2i} are the undetermined out-of-plane nodal displacement parameters along the edges of the strip and $\eta=y/b_s$ and $\xi=\pi/a$. The investigation on the sensitivity of the full-energy FSM analysis to the number of harmonic terms revealed that the fundamental frequency of FML plates can be predicted with a very good accuracy by using three first harmonic terms (i.e. $i=1,2,3$ in Eq. (15)).

3. Particle swarm optimization algorithm

Eberhart and Kennedy (1995) first presented a standard PSO algorithm, which is inspired by the social behavior of bird flocks or fish schools. Similar to GAs, a PSO algorithm is a population-based algorithm. A population of candidate solutions is called a particle swarm. This method is used to search for the global optimum of wide variety of arbitrary problems. In a GA, each of the

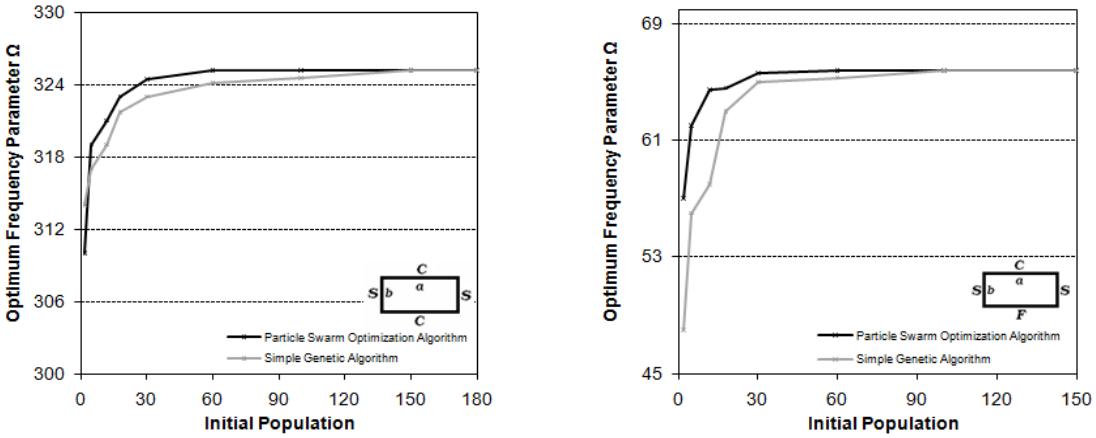

Fig. 2 Comparison of the PSO and GA results for SCSC and SCSF edge conditions for symmetrically FML 10-layered rectangular (*a/b=2*) panels with the same generations.

three main classes of operations (selection, crossover, and mutation) can be implemented in a number of ways. PSO does not label its operations in the same way as GAs, but analogies exist. These analogies depend, of course, on the implementation of the GA operation. In PSO, instead of using more traditional genetic operators, each particle (individual) adjusts its "flying" according to its own flying experience and its companions' flying experience. Complicating any comparisons is the fact that the effects of the various operations often vary over the course of a run (Eberhart and Shi 1998). PSO is initialized with a group of random particles and then searches for optima by updating generations.

In each iteration, the swarm is updated using the following equations

$$v_k^i = wv_{k-1}^i + c_1 r_1 (p^i - x_{k-1}^i) + c_2 r_2 (p_{k-1}^g - x_{k-1}^i) \tag{16}$$

$$x_k^i = x_{k-1}^i + v_k^i \tag{17}$$

where x^i and v^i represent the current position and the velocity of the i^{th} particle respectively; p^i is the best previous position of the ith particle (called pbest) and p^g is the best global position among all the particles in the swarm (called gbest); r_1 and r_2 are uniformly distributed random numbers in the interval [-1 1], c_1 and c_2 are the acceleration constants and w is the inertia weight for velocities that control the impact of the previous history of velocities on the current velocity, thereby influencing the trade-off between global (wide-ranging) and local (fine-grained) exploration abilities of the flying points. A larger inertia weight facilitates global exploration (searching new areas) while a smaller inertia weight tends to facilitate local exploration to free-tune the current search area. Suitable selection of the inertia weight provides a balance between global and local exploration abilities and thus requires fewer iterations on average to find the optimum. In this work, $c_1=c_2=1$ and $w=0.75$ are chosen which give better optimal results in lesser iterations, and the results also are rounded to nearest integer values after optimization. A simply way to understand this updating procedure is depicted by Hassan *et al*. (1897). Also the performance of the PSO algorithm can be improved by using modification strategies or hybrid techniques (Sepehri *et al*. 2012, kaveh and Talatahari 2012, Erdal *et al*. 2013).

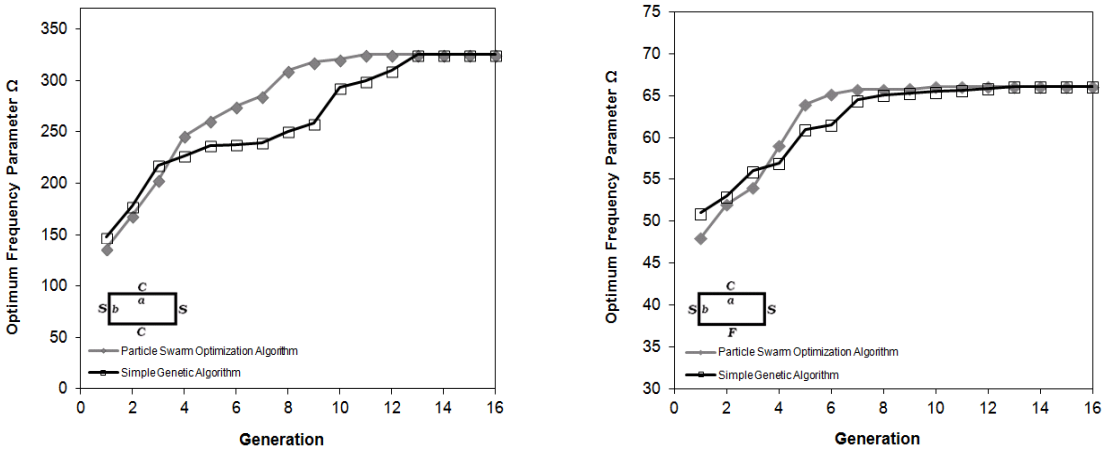

(a) (b)

Fig. 3 Comparison of the PSO and GA results for SCSC and SCSF edge conditions for symmetrically FML 10-layered rectangular (*a/b=2*) panels with the same initial populations.

The performance of the PSO is shown in Fig. 2(a) and (b) in comparison with the simple GA with the same generations and it shows the good efficiency of the PSO algorithm. In the 10 layered cases, the optimal values for PSO and GA converge in around the initial population of 37 and 90, respectively. Also in the 6 layered cases, the optimal values converge in around the initial population 22 and 34 for PSO and GA, respectively The GA parameters such as crossover rate and mutation rate are selected to be 0.6 and 0.02, respectively.

Also the convergence rate of objective function with the number of generations for PSO and GA for symmetrically FML 10-layered rectangular (*a/b=2*) panels is shown in Fig. 3(a) and (b). It is clear from Fig. 3(a) and (b) that, for the optimization problem considered, PSO converges at a faster rate (around 10 generations) compared to that for GA (around 13 generations) with the same initial populations. In the FML 6 layered cases, the optimal values converge in the around generation of 5 and 7 for PSO and GA, respectively. In addition, it is concluded that using of PSO provides a much higher convergence and reduced the CPU time in comparison with the GA.

The training phase elapsed a CPU time of 3–5 min. on a Intel Core i3 2.13GHz CPU speed and 4 Gbyte RAM for the FML 6 layered cases. This time was 15-20 min for the 10 layered cases.

4. Results and discussions

The fundamental frequency of hybrid laminates is maximized for different panel aspect ratio, ply angles, number of layers and boundary conditions. The laminates are symmetric and made of AS/3501 graphite/epoxy material (Vinson and Sierakowski 1986) (inner composite layers) and aluminum alloy 2024-T3 (Shooshtari and Razavi 2010) (outer aluminum layers). The material properties of the laminas are given as below:

Composite layers: $E_1=138$ GPa, $E_2=8.96$ GPa, $G_{12}=7.1$ GPa, $\upsilon_{12}=0.3$

Aluminum layers: $E=72.4$ GPa, $\upsilon=0.33$

Each of the lamina is assumed to be same thickness.

In the previous work (Ghashochi Bargh and Sadr 2012) optimization of composite laminated

Table 1 Dimensionless frequencies of rectangular Glare 3 hybrid composite (*h/ a =0.01*)

BCs	α /b	Ω	
		Shooshtari and Razavi 2010	Present study
SSSS	1	19.4723	19.541
	4/3	26.9917	27.135
	2	48.5124	48.597

panels using PSO algorithm is validated by Narita (2003). The validated code is employed for FML panel structures optimization. It is also seen in Table 1 that there is a very good agreement between results of present approach and the published paper (Shooshtari and Razavi 2010), for the fundamental frequency of symmetric FML panels (Glare 3). The layup and material properties of this hybrid composite (Glare 3) are (Shooshtari and Razavi 2010):

Al(2024-T3)/[0^0/90^0]GFRC/Al(2024-T3)/[90^0/0^0]GFRC/Al(2024-T3)

Glass fiber reinforced composite layers (0.2 mm thickness each): E_1=*55.8979* GPa, E_2=*13.7293* GPa, G_{12}=*5.5898* GPa, υ_{12}=*0.277*, ρ=*2550* kg/m^3

Aluminum alloy 2024-T3 layers (0.3 mm thickness each): *E=72.4* GPa, υ=*0.33*, ρ=*2700* kg/m^3

Dimensionless fundamental frequency of Glare 3 is obtained by using the following equation

$$\Omega = \omega a^2 \left(\frac{I_0}{D_{11}}\right)^{1/2} \tag{18}$$

where $I_0 = \int_{-\frac{h}{2}}^{\frac{h}{2}} \rho dz$ is the mass moment of inertia.

The present optimal stacking sequences and corresponding maximal natural frequencies are compared with those of typical stacking sequences of symmetrical ten-layered FML composite plates, namely $[Al/0/0/0/0]_S$, $[Al/30/-30/30/-30]_S$, $[Al/45/-45/45/-45]_S$, and $[Al/0/90/0/90]_S$ in Fig. 4 and 5. Comparisons demonstrate the present optimal solutions for all various aspect ratios have higher frequencies than the panels with other lay-ups. As inferred from the results, PSO predicts successfully the maximal natural frequency parameters and optimal layered sequences. The natural frequencies of the fiber metal laminated panels are increased with increasing a/b ratios.

The optimal layered sequences and maximal natural frequency parameters of symmetric FML panels are searched using PSO for the various combinations of free (F), simply supported (S) and clamped (C) edge conditions, the panel length/width ratios (*a/b=1,2,3,4*), the layer number (*n= 6,10*), and are given in Tables 2 and 3. The fiber angle of each inner ply in the FML composite panels is changed with a step of $\Delta\theta=1^0$ between ($-90^0 \le \theta_n \le 90^0$). As seen, the optimal fiber orientations vary from 0^0 to 90^0 or 0^0 to -90^0 with increase in a/b ratios and are associated with a smooth transitional region for the case of simply supported panels, such as SSCF. For the case of clamped panels, the optimal fiber orientations change from 0^0 to 90^0 or 0^0 to -90^0 in a sudden manner which occurred at *a /b* ratio of unity, such as CCCC. As inferred from the results, the edge conditions play an important role on the natural frequency parameter of the FMLs. As the number of the clamped panel edges is increased an evident increase in the natural frequency parameters is observed, such as Ω=*75.870* for the edge condition CFCF whereas the Ω=*102.103* for the edge condition CCCC in 6-layerd panel (*a/b=1*). This can be explained that the clamped edges provide less degrees of freedom and it is effective to stiffen the plates.

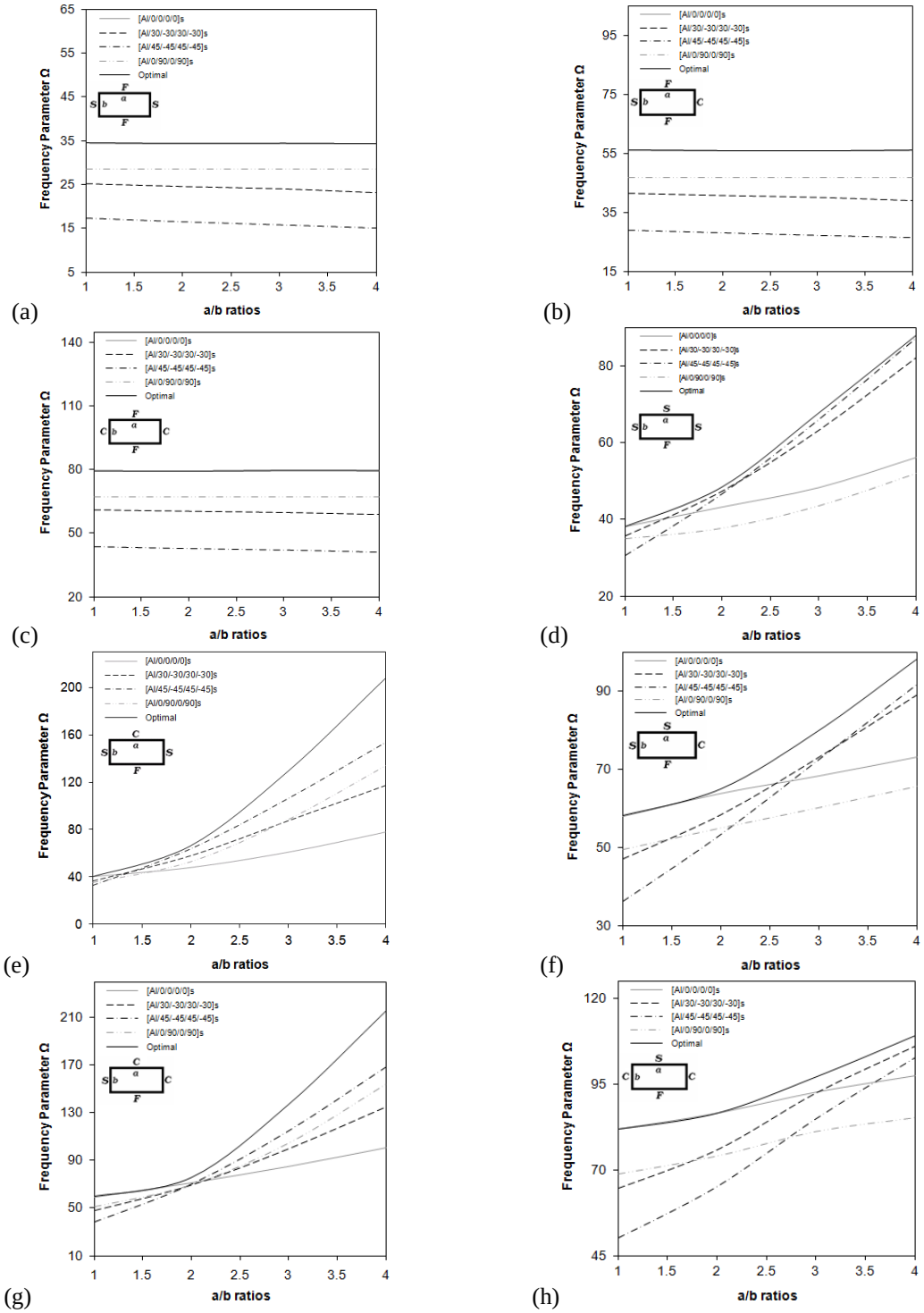

Fig. 4 Comparison between the optimal natural frequency parameters Ω_{opt} and natural frequency parameter of symmetric FML ten-layered panels for various stacking sequences, *a/b* ratios and edge conditions: (a) SFSF, (b) SFCF, (c) CFCF, (d) SSSF, (e) SCSF, (f) SSCF, (g) SCCF, (h) CSCF.

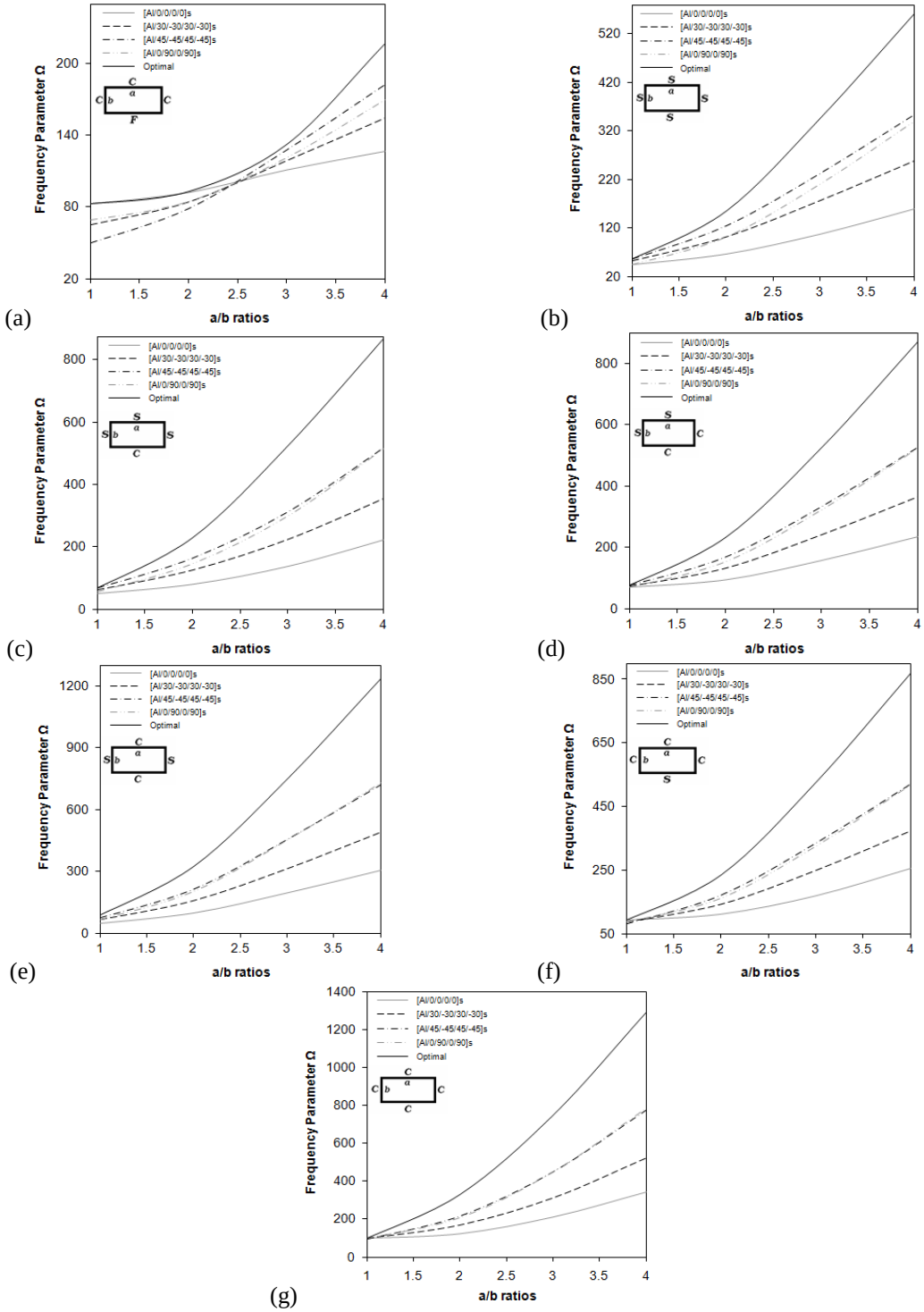

Fig. 5 Comparison between the optimal natural frequency parameters Ω_{opt} and natural frequency parameter of symmetric FML ten-layered panels for various stacking sequences, *a/b* ratios and edge conditions: (a) CCCF, (b) SSSS, (c) SSSC, (d) SSCC, (e) SCSC, (f) CCCS, (g) CCCC

Table 2 Optimum solutions for symmetric 6-layered fiber metal laminated panels

BCs	α /b	$[Al/\theta_1/\theta_2]_{S,opt}$	Ω_{opt}	BCs	α /b	$[Al/\theta_1/\theta_2]_{S,opt}$	Ω_{opt}
SFSF	1	$[Al/0/0]_S$	33.014	CCCF	1	$[Al/0/0]_S$	79.418
	2	$[Al/0/0]_S$	32.961		2	$[Al/0/0]_S$	92.713
	3	$[Al/0/0]_S$	32.925		3	$[Al/-90/89]_S$	132.564
	4	$[Al/0/0]_S$	32.913		4	$[Al/89/90]_S$	215.705
SFCF	1	$[Al/0/0]_S$	52.810	SSSS	1	$[Al/-45/-46]_S$	56.777
	2	$[Al/0/0]_S$	52.621		2	$[Al/-89/90]_S$	154.116
	3	$[Al/0/1]_S$	52.585		3	$[Al/90/88]_S$	343.068
	4	$[Al/0/0]_S$	52.552		4	$[Al/-89/89]_S$	552.521
CFCF	1	$[Al/0/-1]_S$	75.870	SSSC	1	$[Al/60/60]_S$	69.144
	2	$[Al/0/-1]_S$	75.694		2	$[Al/88/-90]_S$	222.937
	3	$[Al/0/0]_S$	76.011		3	$[Al/-90/-89]_S$	520.766
	4	$[Al/0/0]_S$	75.914		4	$[Al/90/90]_S$	858.658
SSSF	1	$[Al/0/0]_S$	36.893	SSCC	1	$[Al/-40/-41]_S$	76.384
	2	$[Al/37/-39]_S$	47.796		2	$[Al/87/90]_S$	229.119
	3	$[Al/42/-46]_S$	65.772		3	$[Al/90/-90]_S$	521.075
	4	$[Al/43/-44]_S$	83.184		4	$[Al/89/-90]_S$	859.639
SCSF	1	$[Al/0/1]_S$	38.748	SCSC	1	$[Al/89/-89]_S$	88.997
	2	$[Al/58/64]_S$	65.319		2	$[Al/89/-90]_S$	312.400
	3	$[Al/90/-89]_S$	128.007		3	$[Al/90/90]_S$	742.618
	4	$[Al/90/-90]_S$	206.413		4	$[Al/90/90]_S$	1218.994
SSCF	1	$[Al/-4/-4]_S$	54.965	CCCS	1	$[Al/0/0]_S$	93.772
	2	$[Al/-19/18]_S$	64.810		2	$[Al/87/90]_S$	231.590
	3	$[Al/-29/46]_S$	77.339		3	$[Al/-90/90]_S$	522.109
	4	$[Al/-38/-40]_S$	95.021		4	$[Al/88/89]_S$	855.732
SCCF	1	$[Al/-5/-5]_S$	56.814	CCCC	1	$[Al/0/2]_S$	102.103
	2	$[Al/-32/-30]_S$	75.361		2	$[Al/-90/90]_S$	320.992
	3	$[Al/87/88]_S$	136.010		3	$[Al/90/-88]_S$	745.334
	4	$[Al/-88/-90]_S$	212.980		4	$[Al/89/90]_S$	1223.418
CSCF	1	$[Al/0/1]_S$	80.116				
	2	$[Al/0/0]_S$	85.218				
	3	$[Al/22/-21]_S$	97.479				
	4	$[Al/34/-32]_S$	106.101				

Tables 2 and 3 also show the effect of number of layers on the optimum design for various panel edge conditions and *a/b* ratios. As seen, the maximum natural frequency and the optimum fiber orientations are not influenced substantially and approach a limiting value with an increasing layer number.

Also fiber orientation angles in the direction with less degree of freedom stiff the plates and increase the fundamental frequency parameters. This is reason that why [Al/0/0]s or [Al/0/0/0/0]s are the optimum lay-ups for the edge conditions SFSF, SFCF and CFCF and [Al/90/90]s or [Al/90/90/90/90]s are the optimum lay-ups for the edge condition SCSC.

Table 4 presents the optimal layered sequences and maximal natural frequency parameters of symmetric 6-layered FML panels with the double-thickness of aluminum layers and the same layer thickness for composite layers as given in Table 2. As inferred from the results, the optimum fiber orientations are not influenced substantially and approach a limiting value with an increasing

Table 3 Optimum solutions for symmetric 10-layered fiber metal laminated panels

BCs	α /b	$[Al/\theta_1/\theta_2/\theta_3/\theta_4]_{S,opt}$	Ω_{opt}	BCs	α /b	$[Al/\theta_1/\theta_2/\theta_3/\theta_4]_{S,opt}$	Ω_{opt}
SFSF	1	$[Al/0/0/1/0]_S$	34.557	CCCF	1	$[Al/0/0/0/0]_S$	82.867
	2	$[Al/0/0/0/2]_S$	34.380		2	$[Al/0/0/0/1]_S$	93.006
	3	$[Al/0/0/0/0]_S$	34.442		3	$[Al/90/-90/89/-90]_S$	132.688
	4	$[Al/0/0/0/0]_S$	34.317		4	$[Al/-90/-88/89/89]_S$	217.115
SFCF	1	$[Al/0/0/0/1]_S$	55.951	SSSS	1	$[Al/-45/-45/-45/44]_S$	56.229
	2	$[Al/0/0/0/0]_S$	55.837		2	$[Al/90/90/-90/90]_S$	154.807
	3	$[Al/0/0/0/0]_S$	55.818		3	$[Al/90/-88/90/-87]_S$	346.044
	4	$[Al/0/0/0/-1]_S$	55.922		4	$[Al/90/-90/89/88]_S$	561.070
CFCF	1	$[Al/0/0/0/-1]_S$	79.366	SSSC	1	$[Al/60/60/60/59]_S$	69.331
	2	$[Al/0/0/0/0]_S$	79.214		2	$[Al/89/-90/90/88]_S$	230.922
	3	$[Al/0/0/0/3]_S$	79.600		3	$[Al/90/90/89/87]_S$	525.538
	4	$[Al/0/0/0/1]_S$	79.483		4	$[Al/89/-90/-88/88]_S$	867.609
SSSF	1	$[Al/0/0/0/0]_S$	38.003	SSCC	1	$[Al/-40/-40/-41/44]_S$	76.390
	2	$[Al/37/37/-37/-37]_S$	48.376		2	$[Al/90/88/-90/90]_S$	232.683
	3	$[Al/-41/44/-44/43]_S$	67.801		3	$[Al/90/90/89/89]_S$	525.755
	4	$[Al/44/-44/45/45]_S$	88.031		4	$[Al/90/90/90/-90]_S$	870.410
SCSF	1	$[Al/0/0/0/-2]_S$	39.323	SCSC	1	$[Al/90/90/-89/-88]_S$	89.114
	2	$[Al/58/58/63/67]_S$	66.118		2	$[Al/90/-90/-87/90]_S$	325.548
	3	$[Al/90/-88/-90/90]_S$	129.554		3	$[Al/-90/90/-90/-89]_S$	747.503
	4	$[Al/90/90/90/-88]_S$	208.195		4	$[Al/90/89/-88/-90]_S$	1232.896
SSCF	1	$[Al/-4/-4/-5/-8]_S$	58.120	CCCS	1	$[Al/0/0/0/-2]_S$	93.988
	2	$[Al/-19/19/17/18]_S$	64.936		2	$[Al/-90/90/88/90]_S$	236.130
	3	$[Al/-32/42/41/-33]_S$	79.866		3	$[Al/90/90/-90/88]_S$	526.663
	4	$[Al/-40/40/-39/38]_S$	98.107		4	$[Al/90/90/90/89]_S$	868.865
SCCF	1	$[Al/-5/-5/-7/-6]_S$	59.774	CCCC	1	$[Al/0/0/1/1]_S$	100.866
	2	$[Al/-32/-32/-31/-30]_S$	75.655		2	$[Al/90/-90/89/88]_S$	331.749
	3	$[Al/88/-89/87/88]_S$	137.202		3	$[Al/-90/-90/90/87]_S$	749.668
	4	$[Al/90/-89/89/-90]_S$	214.233		4	$[Al/90/90/89/89]_S$	1238.084
CSCF	1	$[Al/0/0/1/3]_S$	81.896				
	2	$[Al/0/0/0/1]_S$	86.510				
	3	$[Al/22/-22/23/-22]_S$	97.007				
	4	$[Al/-34/35/35/33]_S$	108.890				

Table 4 Optimum solutions for symmetric 6-layered fiber metal laminated panels with double-thickness aluminum layers

BCs	α /b	$[Al/\theta_1/\theta_2]_{S,opt}$	Ω_{opt}	BCs	α /b	$[Al/\theta_1/\theta_2]_{S,opt}$	Ω_{opt}
SFSF	1	$[Al/0/0]_S$	26.107	SFCF	1	$[Al/0/0]_S$	42.184
	2	$[Al/0/0]_S$	25.790		2	$[Al/0/0]_S$	42.167
	3	$[Al/0/0]_S$	25.868		3	$[Al/0/0]_S$	42.153
	4	$[Al/0/1]_S$	25.844		4	$[Al/0/0]_S$	42.131
CFCF	1	$[Al/0/0]_S$	60.240	SSSF	1	$[Al/0/0]_S$	30.697
	2	$[Al/0/0]_S$	60.117		2	$[Al/37/-38]_S$	40.355
	3	$[Al/0/0]_S$	60.395		3	$[Al/41/-44]_S$	56.968
	4	$[Al/0/0]_S$	60.288		4	$[Al/43/-43]_S$	71.037
SCSF	1	$[Al/0/0]_S$	32.947	SSCF	1	$[Al/-4/-4]_S$	45.793
	2	$[Al/58/63]_S$	55.868		2	$[Al/-19/17]_S$	54.666
	3	$[Al/90/90]_S$	104.706		3	$[Al/-30/44]_S$	65.911
	4	$[Al/90/-90]_S$	171.053		4	$[Al/-38/-41]_S$	82.542

Table 4 Continued

SCCF	1	$[Al/-5/-4]_S$	47.453	CSCF	1	$[Al/0/1]_S$	69.887
	2	$[Al/-31/-31]_S$	60.832		2	$[Al/0/0]_S$	73.089
	3	$[Al/-87/90]_S$	106.709		3	$[Al/22/-23]_S$	84.113
	4	$[Al/89/-90]_S$	175.956		4	$[Al/34/-34]_S$	93.485
CCCF	1	$[Al/0/0]_S$	69.005	SSSS	1	$[Al/45/45]_S$	47.389
	2	$[Al/0/0]_S$	81.243		2	$[Al/90/-90]_S$	129.499
	3	$[Al/-89/89]_S$	103.332		3	$[Al/89/88]_S$	263.052
	4	$[Al/-90/-90]_S$	177.401		4	$[Al/-89/-90]_S$	450.223
SSSC	1	$[Al/60/60]_S$	59.256	SSCC	1	$[Al/-41/-42]_S$	67.758
	2	$[Al/90/90]_S$	184.473		2	$[Al/-88/89]_S$	188.109
	3	$[Al/90/-90]_S$	392.975		3	$[Al/88/90]_S$	392.822
	4	$[Al/88/-90]_S$	685.330		4	$[Al/89/-90]_S$	686.034
SCSC	1	$[Al/-90/90]_S$	75.618	CCCS	1	$[Al/1/0]_S$	81.854
	2	$[Al/-89/-90]_S$	255.547		2	$[Al/-87/89]_S$	189.660
	3	$[Al/88/88]_S$	558.274		3	$[Al/87/90]_S$	393.267
	4	$[Al/-90/89]_S$	982.570		4	$[Al/88/89]_S$	685.143
CCCC	1	$[Al/0/0]_S$	90.008				
	2	$[Al/90/89]_S$	261.240				
	3	$[Al/90/90]_S$	559.717				
	4	$[Al/-90/-90]_S$	986.016				

aluminum layers thickness. Also as seen, with increase in the aluminum layers thickness, the fundamental frequency decreases for a symmetric FML panel.

5. Conclusions

In this study, the layer optimization was carried out for maximizing the fundamental (first) frequency of symmetrical FML panels by the PSO algorithm, and it was numerically demonstrated that the present optimum fundamental frequencies are actually higher than panels with any of typical lay-ups and are equivalent to the global solutions. The natural frequencies of the FML composite panels also were calculated using the finite strip technique for various plate edge conditions, length/width ratios, thickness of metal sheets and layer number. The present method finds optimal design maximizing the natural frequency of the FML composite panels without yielding a local optimum for all edge conditions and design parameters whereas this possibility is experienced in the Ritz-based layerwise optimization method. In addition, the maximum fundamental frequency and the optimum stacking sequences were substantially influenced for edge conditions and a/b ratios. As seen, the maximum fundamental frequency and the optimum fiber orientations were not substantially influenced and approach a limiting value with an increasing layer number.

References

Aksoylar, C., Omercikoglu, A., Mecitoglu, Z. and Omurtag, M.H. (2012), “Nonlinear transient analysis of

FGM and FML plates under blast loads by experimental and mixed FE methods", *Compos Struct*., **94**, 731-44.
Apalak, M.K., Yildirim, M. and Ekici, R. (2008), "Layer optimisation for maximum fundamental frequency of laminated composite plates for different edge conditions", *Composites Science and Technology*, **68**, 537-50.
Bert, C.W. (1977), "Optimal design of a composite material plate to maximise its fundamental frequency", *Journal of Sound and Vibration*, **50**, 229-37.
Bert, C.W. (1978), "Design of clamped composite plates to maximise fundamental frequency", *Journal of Mechanical Design*, **100**, 274-8.
Bloomfield, M.W., Diaconu, C.G. and Weaver, P.H. (2009), "On feasible regions of lamination parameters for lay-up optimization of laminated composites", *Proceedings of the Royal Society of London, Series A (Mathematical, Physical and Engineering Sciences)*, **465**(2104),1123-43.
Eberhart, R.C. and Kennedy, J. (1995), "A new optimizer using particle swarm theory", *Proceedings of the Sixth International Symposium on Micro Machine and Human Science*, IEEE Service Center, Piscataway, NJ, Nagoya, Japan.
Eberhart, R.C. and Shi, Y. (1998), "Comparison between genetic algorithms and Particle Swarm Optimization", (Eds. Porto, V.W., Saravanan, N., Waagen, D. and Eiben, A.E.), *Evolutionary Programming VII*, Springer.
Erdal, F., Doğan, E. and Saka, M.P. (2013), "An improved Particle Swarm Optimizer for steel grillage systems", *Structural Engineering and Mechanics*, **47**(4), 513-30.
Fukunaga, H. and Hideki Sekine, H. (1992), "Stiffness design method of symmetric laminates using lamination parameters", *AIAA Journal.*, **30**(11), 2791-3.
Ghashochi Bargh, H. and Sadr, M.H. (2011), "Optimal design by Elitist-Genetic algorithm for maximum fundamental frequency of fiber metal laminated plates", *Key Engineering Materials*., **471-72**, 331-6.
Ghashochi Bargh, H. and Sadr, M.H. (2012), "Stacking sequence optimization of composite plates for maximum fundamental frequency using particle swarm optimization algorithm", *Meccanica*, **47,** 719-30.
Grenestedt, J.L. and Gudmundson, P. (1993), "Lay-up optimisation of composite material structures", *Proceedings of the IUTAM Symposium on Optimal Design with Advanced Materials*, Lyngby, Denmark.
Gürdal, Z., Haftka, R.T. and Hajela, P. (1999), *Design and optimisation of laminated composite materials*, John Wiley and Sons, New York.
Hassan, R., Cohanim, B. and Weck, O. (2005), "A comparison of particle swarm optimization and the genetic algorithm", *Proceedings of the 46th AIAA/ASME/ASCE/AHS/ASC Structures, Structural Dynamics & Material Conference*, No. 1897, Austin, Texas.
Jones, R.M. (1975), *Mechanics of Composite Materials*, Scripta, Washington, DC.
Kam, T.Y. and Chang, R.R. (1993), "Design of laminated composite plate for maximum buckling load and vibration frequency", *Comput Methods Appl Mech Eng*., **106**, 65-81.
Kaveh, A. and Talatahari, S. (2012), "A hybrid CSS and PSO algorithm for optimal design of structures", *Structural Engineering and Mechanics*, **42**(6), 783-97.
Kennedy, J. and Eberhart, R.C. (1995), "Particle swarm optimization", *Proc. IEEE Int'l Conf on Neural Networks*, IEEE Service Center, Piscataway, NJ.
Mateus, H.C., Soares, C.M.M. and Soares, C.A.M. (1991), "Sensitivity analysis and optimal design of thin laminated composite structures", *Computers and Structures*, **41**, 501-8.
Narita, Y. (2003), "Layerwise optimization for the maximum fundamental frequency of laminated composite plates", *J. Sound and Vibration*, **263**, 1005-16.
Reiss, R. and Ramachandran, S. (1987), "Maximum frequency design of symmetric angle-ply laminates", (Ed. Marshall, I.H.), *Composite Structures: Analysis and Design Studies*, **1**(4), 1476-87.
Sadr, M.H. and Ghashochi Bargh, H. (2010), "Fundamental frequency optimization of angle-ply laminated plates using Elitist-Genetic algorithm and finite strip method", *Proceedings of the ASME 10th Biennial Conference on Engineering Systems Design and Analysis*, Istanbul, Turkey.
Sadr, M.H. and Ghashochi Bargh, H. (2011), "Fundamental frequency optimization of laminated cylindrical panels by Elitist-Genetic algorithm", *Key Engineering Materials*., **471-472**, 337-42.

Sadr, M.H. and Ghashochi Bargh, H. (2012), "Optimization of laminated composite plates for maximum fundamental frequency using Elitist-Genetic algorithm and finite strip method", *J Glob Optim.*, **54**, 707-28.

Sepehri, A., Daneshmand, F. and Jafarpur, K. (2012), "A modified Particle Swarm approach for multi-objective Optimization of laminated composite structures", *Structural Engineering and Mechanics*, **42**(3), 335-52.

Shooshtari, A. and Razav,i S. (2012), "Stability and bifurcation analysis of symmetric laminated composite and fiber metal laminated plates in steady-state motion", *Information Engineering Letters*., **2**, 37-43.

Shooshtari, A. and Razavi, S. (2010), "A closed form solution for linear and nonlinear free vibrations of composite and fiber metal laminated rectangular plates", *Composite Structures.*, **92**, 2663-75.

Tsai, S.W. and Pagano, N.J. (1968), "Invariant Properties of Composite Materials, in Composite Materials", *Composite Materials Workshop*, Tehnomic Pub. Co., 233-53.

Vinson, J.R. and Sierakowski, R.L. (1986), *The Behavior of Structures Composed of Composite Materials*, Martinus Nijhoff, Dordrecht.